J Solution Chem (2009) 38: 1267–1282
DOI 10.1007/s10953-009-9445-9

Aqueous Long-Term Solubility of Titania Nanoparticles and Titanium(IV) Hydrolysis in a Sodium Chloride System Studied by Adsorptive Stripping Voltammetry

Jochen Schmidt · Wolfram Vogelsberger

Received: 8 December 2008 / Accepted: 26 March 2009 / Published online: 3 September 2009

Abstract The solubility of industrially produced titanium dioxide nanoparticles has been studied in aqueous sodium chloride media in the pH range 1 to 13 at 25 °C by using adsorptive stripping voltammetry (AdSV). Kinetic dissolution curves have been obtained as well as long-term solubilities that provide an approximation of the equilibrium solubilities. The titania nanoparticles used in the dissolution experiments have been characterized by nitrogen sorption measurements, XRD and colloid titration. The equilibrium solubilities and titanium(IV) speciation and their dependences on pH have been modelled by assuming the formation of the mononuclear titanium hydroxo complexes $[Ti(OH)_n]^{(4-n)+}$ ($n = 2$ to 5) to be the only titanium species present. The solubility product of titanium dioxide and equilibrium constants for titanium(IV) hydrolysis, calculated from the AdSV solubility data, are presented.

Keywords Titania · Nanoparticles · Dissolution · Titanium(IV) hydrolysis · Adsorptive stripping voltammetry of Ti(IV)

1 Introduction

Titania is used in many applications in technology and everyday life because of its excellent dielectric and chemical properties [1–3]. With the increasing use and synthesis of nanomaterials, questions arise on the stability of nanostructures as well as on the toxicity

Electronic supplementary material The online version of this article (http://dx.doi.org/10.1007/s10953-009-9445-9) contains supplementary material, which is available to authorized users.

J. Schmidt (✉) · W. Vogelsberger
Institute of Physical Chemistry, Chemistry and Earth Science Faculty, Friedrich-Schiller-University Jena, Helmholtzweg 4, 07743 Jena, Germany
e-mail: j.schmidt@lfg.uni-erlangen.de

J. Schmidt
Institute of Particle Technology, University of Erlangen-Nuremberg, Cauerstrasse 4, 91058 Erlangen, Germany

of nanoparticles [4–6], and thus dissolution phenomena of ultrafine particles need to be investigated. Moreover, during synthesis knowledge about solubility and aqueous chemistry provide crucial parameters to control particle size, particle shape and phase or aggregation behavior [7–13]. It can be seen from these different considerations that reliable information about the dissolution kinetics as well as the equilibrium solubility of even sparingly soluble matter like titanium dioxide, and the effects particle size on solubility in general [14–16], needs to be established.

In aqueous media (pH > 1) at ambient temperature, crystalline bulk titanium dioxide shows very small equilibrium solubilities that only can be quantified by means of trace analysis. Perhaps as a result there are only a few recent publications that deal with the experimental determination of the aqueous solubility of titania or hydrous titanium oxide under rather moderate dissolution conditions [11, 14, 17, 18]. At geologically relevant conditions, i.e. at high pressure and high temperature, data are also available on the solubility of titania (see, e.g. refs. [19–21]).

Ziemniak et al. performed solubility measurements of rutile in the temperature range 17 °C to 288 °C with an autoclave flow system at alkaline pHs in aqueous sodium phosphate, sodium hydroxide and ammonia solutions [17]. They found nanomolal to micromolal titanium(IV) solubilities under these alkaline conditions and give in their article comprehensive thermochemical parameters for the TiO_2–H_2O system. The quantitative titanium determinations have been performed with AAS after preconcentration of the sample solutions.

More recently, Knauss et al. studied the solubility of rutile over a broad pH range from pH = 1 to pH = 13 in buffer solutions at temperatures of 100 to 300 °C [18]. They found solubilities measured by ICP-MS of about $10^{-6.3}$ mol·kg^{-1} at pH = 1 (100 °C) and 10^{-7} mol·kg^{-1} at pH = 2 (100 °C). At pH = 6.5 and 8.5 (100 °C) comparable molal solubilities of about $10^{-7.7}$ mol·kg^{-1} were reported. In accordance with the findings of Ziemniak et al. [17], an increase in titanium(IV) solubility is also observed in the alkaline pH range pH > 11.

Sugimoto et al. [11] studied the solubility of a freshly prepared amorphous titanium oxide by using ICP-OES. While Knauss et al. [18] obtained results like those of Ziemniak et al. [17] for the titania equilibrium solubilities, Sugimoto et al. present solubilities of a freshly precipitated titanium oxide that were several orders of magnitude higher than for the crystalline polymorphs. The increased solubility of freshly precipitated or amorphous oxides or hydrous oxides of titanium is a well-known phenomenon. It is therefore essential to perform a thorough characterization of the solid used in dissolution experiments.

Some results [22, 23] on the formation of aqueous hydroxo complexes of titanium(IV) are contradictory. The characteristics of the solid phase are often not well described and amorphous samples or samples containing a hydrous titanium oxide phase frequently were studied [11, 24].

Due to this rather fragmentary knowledge of the equilibrium solubility of crystalline titanium dioxide at ambient temperatures (25 °C), and especially on the solubility of titania nanoparticles, we decided to perform studies on the dissolution kinetics [14, 15] as well as on the long-term solubilities of industrially produced titanium dioxide nanostructured particles that are reported here. Moreover, the solubility of a hydrous titanium oxide sample has been studied in the acidic pH range in order to demonstrate the effect of hydration/hydroxylation of the solid. These dissolution studies have been carried out in aqueous sodium chloride solutions of pH = 1 to 13 in a closed system. As the formation of titanium chloro complexes [25] and polynuclear titanium complexes [26, 27] under the experimental conditions can be neglected, the aqueous titanium(IV) speciation has been modelled with

only the mononuclear titanium hydroxo complexes $[Ti(OH)_n]^{(4-n)+}$ (where $n = 2, \ldots, 5$), and stepwise and cumulative hydrolysis constants have been derived. The solids have been characterized by XRD, nitrogen sorption measurements and colloid titration. The quantitative analysis of trace amounts of dissolved titanium(IV) has been performed by adsorptive stripping voltammetry (AdSV) in the potassium chlorate–mandelic acid system [28].

2 Experimental

2.1 Setup of Dissolution Experiment and Sampling

All chemicals used, if not otherwise stated, were of special purity, i.e., for trace analysis or puriss p.a. As far as possible glass equipment was not used. Laboratory equipment made of PP, PMP or PTFE were used instead. The dissolution experiments with the industrially produced titanias P25 (Evonik Degussa), DT51D (Millenium Chemicals), G5 (Millenium Chemicals), and with an uncalcined titanium hydrous oxide slurry TRONOX Hydrate Paste (Tronox), were performed in a closed system (50 mL to 500 mL PP or PTFE bottles) at $(25 \pm 1)\,^{\circ}C$. Details on these titanium oxides are given in the "Results and Discussion". The bottles were stored on a shaker (Unimax 1010, Heidolph Instruments) at 150 shakes per minute (switched on daily for at least 8 hours) in an incubation hood. A background electrolyte concentration of 0.1 $mol \cdot L^{-1}$ NaCl was applied, and the pH values were adjusted by the addition of 0.1 $mol \cdot L^{-1}$ to 1 $mol \cdot L^{-1}$ HCl (dilution of 37% HCl Fluka, TraceSelect) or with 0.1 $mol \cdot L^{-1}$ NaOH or concentrated NaOH (Merck, p.a.). A 540 GLP (WTW) pH meter was used for pH measurements. The initial surface area to solvent volume ratio (i.e. the surface area according to the BET method of the sample under consideration exposed to the volume of the electrolyte solution) was fixed at 0.40 $m^2 \cdot mL^{-1}$ in all experiments.

The dispersions were prepared by introducing the appropriate amount of solid titania (dried at 110 °C) into the electrolyte solution at pre-adjusted pH and temperature while stirring at 400 revolutions per minute (magnetic stirring device). Right after addition of the solid, the pH value was adjusted and the bottle was transferred into the incubation hood.

The following sampling procedure was applied: after dissolution times of at least 500 hours (for long-term solubility data) samples of up to 10 mL of the dispersion were withdrawn. The solid residue was separated from the sample solution to be analyzed by centrifugation (10 minutes at 4100 rotations per minute with a Z320 device (Hermle)) and then by filtration (cellulose acetate, 0.2 µm, Schleicher and Schuell). No particles could be detected within the filtered solution as confirmed by dynamic light scattering measurements (DLS). The filtered sample solutions with $pH \leq 2$ were stored in PP bottles without altering the pH. The less acidic filtered sample solutions up to $pH = 7$ were adjusted to $pH = 2$ by addition of HCl before storage, in order to prevent the formation of polymeric species and precipitation. Samples having alkaline pH were stored at the solution pH value. The pH necessary for the AdSV determination ($pH = 3.3$) was adjusted in the presence of mandelic acid just before the measurement. Whenever possible, the AdSV titanium determinations were performed within one day after sampling.

2.2 Adsorptive Stripping Voltammetry (AdSV)

AdSV was the preferred determination method. The reliability of the results of the AdSV method was established by comparison to ICP-MS measurements [14]. The advantage of AdSV compared to ICP-MS is that particles possibly not removed by filtration are detected

Table 1 (**a**) Instrumental parameters and composition of the electrolyte system for the determination of Ti(IV) by AdSV; and (**b**) determination of standard sample solutions

System parameters	Parameter value
(a)	
Deposition potential (versus Ag/AgCl)/mV	−570
Deposition time/s	60
HMDE surface area/mm^2	0.68
Pulse amplitude/mV	60
Pulse time/s	0.1
Sweep rate/$mV \cdot s^{-1}$	40
Temperature of voltammetric cell/°C	(25 ± 1)
Composition of supporting electrolyte	54.6 $mmol \cdot L^{-1}$ $KClO_3$ 4.8 $mmol \cdot L^{-1}$ mandelic acid 2.7 $mmol \cdot L^{-1}$ ammonia
Titanium(IV) in sample solution (target)/$nmol \cdot L^{-1}$	Titanium(IV) in sample solution (actual)/$nmol \cdot L^{-1}$
(b)	
1.82	1.80 ± 0.11
4.56	4.40 ± 0.12

as increased titanium content by ICP-MS. In contrast, it has been proven experimentally that AdSV works well even in the presence of relatively large amounts of colloid particles [29]. Quantification of the titanium(IV) concentrations in the solutions was performed by adsorptive stripping voltammetry (AdSV) in mandelic acid–$KClO_3$ solutions, using a VA Computrace 757 device (Metrohm) in the DP-Mode. Reduction of the titanium(IV)–mandelic acid complex is evaluated and the signal is enhanced by a catalytic current [28]. A hanging mercury drop electrode (HMDE) was used as the working electrode. The voltammetric parameters applied and the composition of the supporting electrolyte are summarized in Table 1(a). The standard addition method (three additions, threefold replications) was used. If necessary, the pH was adjusted to 3.0–3.3 by addition of NH_3 or HCl. The peak current, corrected for the baseline determined by a blank measurement, has been evaluated using VA Computrace 1.0 software. All reagents applied were suprapure or puriss p.a. in order to minimize analytical blanks. The detection limit of the method by applying the parameters summarized in Table 1 was found to be 0.026 ppb as calculated from calibration graphs. The reproducibility and accuracy of the method was tested by the determination of standard sample solutions (see Table 1(b)).

2.3 XRD Investigations

Diffraction patterns of the samples were recorded with an URD-6 (Freiberger Präzisionsmechanik) device at a resolution of 0.01° for $8° \leq 2\Theta \leq 60°$. Mo K-α radiation was used. Evaluation of the data was done with the software Powder Cell 2.4 [30] by simulation of the diffraction pattern using pseudo Voigt functions and single crystal data from the Inorganic Crystal Structure Database (ICSD) (rutile: ICSD collection code no. 31322; anatase: no. 31064; brookite: no. 36408). The composition of the samples as well as the mean crystallite diameter have been obtained.

2.4 Gas Sorption Measurements

Nitrogen sorption isotherms of the titania powders were obtained with a volumetric sorption analyzer Autosorb-1 (Quantachrome). In a typical experiment about 200 to 500 mg of the powder were first outgassed at 350 °C for at least 2 h. Then adsorption and desorption isotherms were recorded at 77 K. The evaluation of this data was done with the Autosorb 1.0 software (Quantachrome).

2.5 Colloid Titration

Titrations of aqueous dispersions of the powder were performed in order to obtain information about the point of zero charge (pzc). A mass of substance corresponding to 20 m^2 BET surface area was transferred to a vessel of the titration device TR250/Titronic T110 (Schott). 60 mL of NaCl solution (0.001 $mol \cdot L^{-1}$ to 0.1 $mol \cdot L^{-1}$) was added and a magnetic stirring bar was used to disperse the powder. The dispersion was continuously purged with argon for about 15 minutes prior to and during the titration. The pH was adjusted to 9.5 by addition of Ar-purged NaOH (0.1 $mol \cdot L^{-1}$, volumetric standard, Aldrich). Then, a titration was performed with HCl (0.1 $mol \cdot L^{-1}$, volumetric standard, Aldrich) until a final pH < 3 was obtained. Then, a blank measurement for a NaCl solution (without solid), after addition of the same amount of NaOH (Ar-purged) as in the preceding measurement, was performed. From these two measurements, surface charge density versus pH curves can be calculated and the pzc is obtained. Intrinsic dissociation constants of surface hydroxyls of titania have been determined from these data by applying the procedure described by Barringer et al. [31].

3 Results and Discussion

3.1 Characteristics of Titania Nanoparticle Samples

The results on phase composition and specific surface area are summarized in Table 2. The mean crystallite diameter and the average particle diameter determined from the BET surface area d_{BET} provide a rough estimate of the primary particle size within larger nanostructured units. All titanias under consideration are large scale products used as, e.g., filler components or catalysts, and are of pure anatase phase, a mixture of anatase and rutile, or a mixture of anatase and an amorphous phase. They were produced either by flame pyrolysis (P25, Evonik Degussa) or by precipitation (DT51D and G5, Millenium Chemicals). For comparison, the solubility of an un-calcined titanium hydrous oxide slurry (TRONOX Hydrate Paste, Tronox) was also determined. The solid content of the slurry was washed by repeated centrifugation in deionized water and dried at 110 °C overnight, prior to its characterization and use in the dissolution experiment.

XRD (see Fig. 1) reveals that the samples DT51D and G5 are phase pure anatase, whereas P25 is a mixture of anatase and rutile. According to our XRD results, the titanium hydrous oxide sample TRONOX is composed of larger anatase crystallites of about 11 nm in diameter and smaller anatase crystallites < 5 nm. The fraction of these small crystallites has been defined as an X-ray amorphous anatase phase (crystallites < 5 nm). The mass fractions have been obtained by simulation of the XRD patterns with the software Powder Cell using single crystal data of anatase. The amorphous phase was simulated by using a widened profile function of the anatase pattern. The crystallite diameters reported have been calculated according to the Scherrer equation from the X-ray pattern.

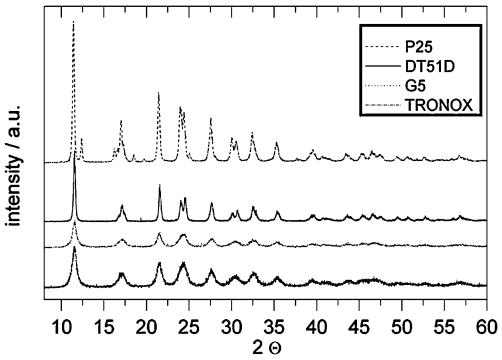

Fig. 1 XRD patterns of different industrially produced titania and titanium hydrous oxide samples

Table 2 Phase composition (XRD) and BET surface area (nitrogen sorption, 77 K) of different titanium dioxide nanoparticles and titanium hydrous oxide

Sample	Phase composition (XRD)/phase (wt.-%)	Crystallite diameter/ nm	BET surface area $S_{BET}/m^2 \cdot g^{-1}$; (correlation coefficient of BET evaluation)	Micropore surface area (t-method)/ $m^2 \cdot g^{-1}$	Mean particle diameter calculated from BET surface area d_{BET}/nm
P25 (Evonik Degussa)	anatase (86) rutile (14)	24.4 (anatase) 29.7 (rutile)	55.7 ($R^2 = 0.999910$)	–	28.3
DT51D (Millenium Chemicals)	anatase (100)	23.9	88.5 ($R^2 = 0.999944$)	–	17.8
G5 (Millenium Chemicals)	anatase (100)	9.7	332.5 ($R^2 = 0.999755$)	168.7	4.7
TRONOX Hydrate Paste (Tronox)	anatase (29) amorphous (71)	11.3 (anatase) 4.7 (amorphous)	302.5 ($R^2 = 0.999559$)	119.6	5.2

The XRD results are consistent with Raman results (not shown here). The minimum primary particle size is given by the crystallite diameter determined by XRD. For sample P25 the primary particle size evaluated from the BET surface area S_{BET}, by assuming spherical particles of uniform size (see Eq. 1), compares favorably to the crystallite diameter determined by XRD (calculated with Powder Cell 2.4), and the other samples show at least qualitative agreement. This agreement is reasonable because the assumptions made for the determination of a mean particle diameter d_{BET} from the BET surface area strictly only applicable in non-porous samples, whereas DT51D is mesoporous and G5 and TRONOX show micro- and mesoporosity (see Fig. 2). An assumed density ρ of 3.8 $g \cdot cm^{-3}$ has been used to

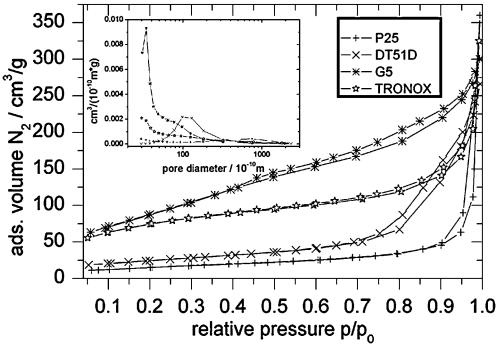

Fig. 2 Nitrogen sorption isotherms of crystalline and hydrous titania samples and desorption pore size distribution (BJH method)

obtain an estimate of d_{BET} (see Eq. 1).

$$d_{\mathrm{BET}} = \frac{6}{S_{\mathrm{BET}}\rho} \tag{1}$$

3.2 Surface Charge Density and Point of Zero Charge

Solubility is strongly influenced by the surface charge of the respective oxide in an aqueous environment [32]. A solid is expected to show minimum solubility in the vicinity of its point of zero charge (pzc). Therefore, the determination of surface charge densities by titration of colloids may provide useful information about the surface charge state and its dependence on pH. Moreover, intrinsic dissociation constants for the surface hydroxyls of TiO_2 can be extracted from these data [31].

The surface charge on titania results, according to the 2 pK-model, from charged surface sites formed by the following protolysis reactions:

$$\equiv \mathrm{Ti} - \mathrm{OH}_2^+ \leftrightarrows \mathrm{Ti} - \mathrm{OH} + \mathrm{H}^+$$

where

$$K_{\mathrm{s},1} = \frac{[\equiv \mathrm{Ti} - \mathrm{OH}][\mathrm{H}^+]}{[\equiv \mathrm{Ti} - \mathrm{OH}_2^+]} = K_{\mathrm{s},1}^0 \exp(Y_0) \tag{2}$$

and

$$\equiv \mathrm{Ti} - \mathrm{OH} \leftrightarrows \mathrm{Ti} - \mathrm{O}^- + \mathrm{H}^+$$

where

$$K_{\mathrm{s},2} = \frac{[\equiv \mathrm{Ti} - \mathrm{O}^-][\mathrm{H}^+]}{[\equiv \mathrm{Ti} - \mathrm{OH}]} = K_{\mathrm{s},2}^0 \exp(Y_0) \tag{3}$$

The equilibrium constants K with superscript 0 represent intrinsic equilibrium constants and Y_0 represents the normalized dimensionless surface potential.

In Fig. 3 are presented surface charge density (σ_0) versus pH curves for the three titanium dioxides studied and an amorphous titanium hydrous oxide (all at 25 °C). It can be clearly seen that the pzc for anatase (DT51D, G5) is found at pH = 5.8 to 6.1 (see Table 3). This result is in agreement with most of the findings in the literature. Kosmulski [33] proposed in his review of the point of zero charge of anatase and rutile that the pzc = 5.9 for both polymorphs. The pzcs calculated as pzc $= 0.5(\mathrm{p}K_{\mathrm{s},1}^0 + \mathrm{p}K_{\mathrm{s},2}^0)$ from the intrinsic dissociation

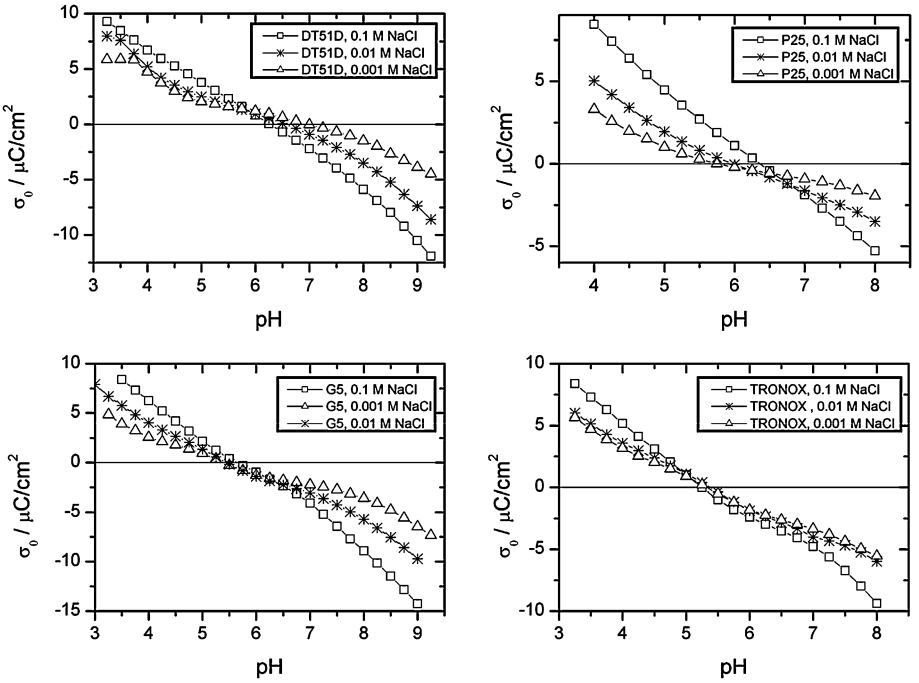

Fig. 3 Surface charge density versus pH plots of crystalline and hydrous titania samples, where M denotes the concentration units mol·L^{-1}

Table 3 The pzc and intrinsic surface hydroxyl dissociation constants of industrially produced titanias and hydrous titanium oxide obtained by colloid titration

Sample	pzc	$pK^0_{s,1}$	$pK^0_{s,2}$
DT51D (anatase)	5.8 ± 0.1	2.5	9.2
G5 (anatase)	6.1 ± 0.3	2.6	9.4
P25 (anatase, rutile)	6.5 ± 0.3	3.2	10.1
TRONOX (amorphous, anatase)	5.3 ± 0.4	2.5	7.9
Literature (Barringer et al. [31])			
Rutile	5.9	2.7	9.1
Anatase	5.95	3.2	8.7
Amorphous titania	5.2	2.0	8.4

constants of surface hydroxyls given by Barringer et al. [31] gives more or less the same values of pzc = 5.9 and 5.95 for anatase and rutile. The pzc found for P25 and TRONOX are slightly higher and lower, respectively, than the value observed for anatase DT51D. A shift to a lower pzc for amorphous titania samples like TRONOX is known to occur. Small deviations in the pzc values can be explained qualitatively by the recently suggested multi-site complexation model [34]. This model explicitly considers different coordinated Ti–O groups in crystalline rutile and anatase. In the framework of this model, a pzc of 5.9 is reported to for rutile, and $\log_{10} K$ values of 7.5 and 4.4 (singly and doubly coordinated surface groups) are obtained. A change in the proportion of these groups is obviously the case for mixtures of the two polymorphs, but it may also play a role if the particles are very

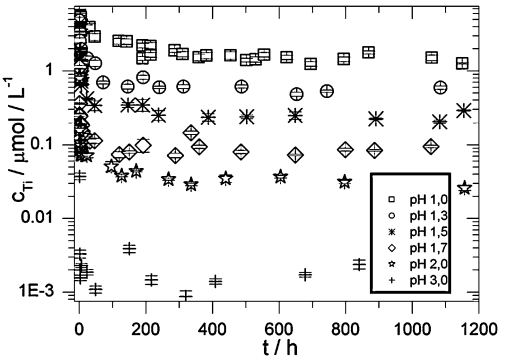

Fig. 4 Dependence of the concentration of dissolved titanium(IV) on the pH and dissolution time {40 m^2 surface area per 100 mL solution of DT51D (anatase); 0.1 mol·L^{-1} NaCl; 25 °C}

small. The intrinsic dissociation constants obtained from our colloid titration data show the qualitative behavior expected for the distinction between amorphous titania and anatase.

3.3 Aqueous Solubility of Anatase Nanoparticles DT51D Its Dependence on Time

The solubilities of DT51D (anatase) nanoparticles in 0.1 mol·L^{-1} NaCl and their dependence on dissolution time are depicted in Fig. 4 for different pH values. It is noteworthy that during the first 70 hours after starting the dissolution experiments, the titanium(IV) concentrations observed exceed the saturation solubilities (dissolution time $>$ 500 h) considerably. This type of behavior was observed earlier for different substances [14–16] and explained within the framework of a phenomenological dissolution model [35] as a kinetic size effect, which is a general characteristic behavior of nanoparticulate matter. The kinetic size effect is not the subject of this paper, for details please see refs. [14–16, 35]. It has been established that for dissolution times greater than 500 hours (see Fig. 4) the amount of dissolved titanium(IV) does not change within the accuracy of the determination method. Therefore, these long-term solubilities (for $\geq$500 h dissolution time) can be used as a good estimate of equilibrium solubility under these dissolution conditions.

3.4 pH Dependence of the Long-term Solubility of Titania Nanoparticles

The aqueous solubilities of the different titania samples for dissolution times longer than 500 hours and their dependence on pH are shown in Fig. 5. First, we note that the pure anatase sample DT51D, the anatase rutile mixture P25, as well as a pure bulk rutile sample (RL11A, Millenium Chemicals) consisting of micron-sized primary particles, and a bulk anatase sample (AT1, Millenium Chemicals; solubility data for RL11A and AT1 not shown here) have comparable long-term solubilities. Only in the case of G5 is there a pronounced size effect on the long-term solubility of anatase in the acidic pH range (see Fig. 5). This behavior can be explained in terms of the dependence of solubility on the particle's curvature (Kelvin equation): small particles show higher solubility compared to larger ones. G5, which exhibits higher aqueous solubility with respect to P25 and DT51D, consists of the smallest primary particles of the anatase phase under consideration in this study.

Lencka et al. [36] argued from thermodynamic data that rutile should be less soluble than anatase, but this behavior was not observed experimentally (there was no significant difference in solubility within the limits of error of the determination method). Rutile is the thermodynamically more stable phase compared to anatase, but one has to keep in mind

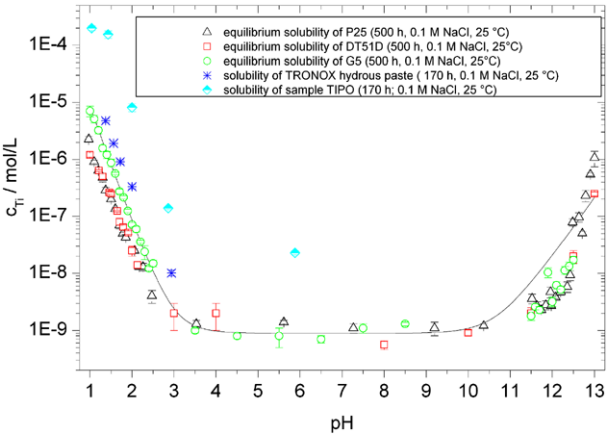

Fig. 5 Solubility of crystalline titania (P25, DT51D, G5) and amorphous titanium hydrous oxides (TRONOX, TIPO) and their dependence on pH (0.1 mol·L^{-1} NaCl; 25 °C) determined by AdSV. *Solid line*: solubility of titanium dioxide ($I = 0.1$ mol·L^{-1}; 25 °C) calculated with the equilibrium constants determined in this study

that the reported Gibbs energies of formation of anatase and rutile do not differ significantly. Therefore, pronounced differences in the solubility of these two polymorphs are not expected.

The long-term solubility data of P25 and DT51D can be used for an appropriate estimate for the bulk equilibrium solubility of titania. In the case of sample G5 the higher determined solubility results from the increased solubility of nanoparticles due to the Kelvin effect.

No significant change in the BET surface areas, i.e. no significant change in mean primary particle size of the titanium dioxide samples DT51D, P25 and G5 exposed to dissolution, was observed within the time frame of the dissolution experiments (see Fig. 6 for a representation of BET surface area dependence on the pH of dissolution and dissolution time; see Table SA in the electronic supplementary material). We also performed SEM studies on sample G5. Possible changes due to dissolution processes, if any, should be noticeable most clearly with this sample. Actually, there are only minor changes of the morphology of the sample G5 (see Fig. SA to SI in the electronic supplementary material).

This is interpreted in terms of the difference in Gibbs energy between the two systems (i.e. the "driving force" for particle growth between titania nanoparticles + electrolyte solution and bulk titania + electrolyte solution), which at this stage of the dissolution process is low. Therefore we can conclude that the long-term solubilities observed for the nanoparticulate titanias P25 and DT51D are not significantly increased above those for bulk titania, although the "real" equilibrium solubilities of bulk titania may be somewhat lower. Nevertheless, our observation that the long-term solubilities of the oxides under consideration and those micron-sized titania are comparable supports the validity of this estimate.

The solubility data were modelled under the assumption that the total pH-dependent concentration of dissolved titanium(IV), $c(\mathrm{Ti})_{\mathrm{total}}(\mathrm{pH})$, is distributed among mononuclear titanium hydroxo complexes of the general formula $[\mathrm{Ti(OH)}_n]^{(4-n)+}$:

$$c(\mathrm{Ti})_{\mathrm{total}}(\mathrm{pH}) = \sum_{n=2}^{5} c[\mathrm{Ti(OH)}_n]^{(4-n)+} \tag{4}$$

In the approach presented by Eq. 4, the species $\mathrm{Ti(OH)}_2^{2+}$, $\mathrm{Ti(OH)}_3^{+}$, $\mathrm{Ti(OH)}_4$ and $\mathrm{Ti(OH)}_5^{-}$ are taken into account. Consideration of higher charged species like $\mathrm{Ti(OH)}^{3+}$ or "Ti^{4+}" in the pH range studied is not necessary as they are not expected to exist under these conditions. Thus, when making calculations according to Eq. 4 when taking into account these species

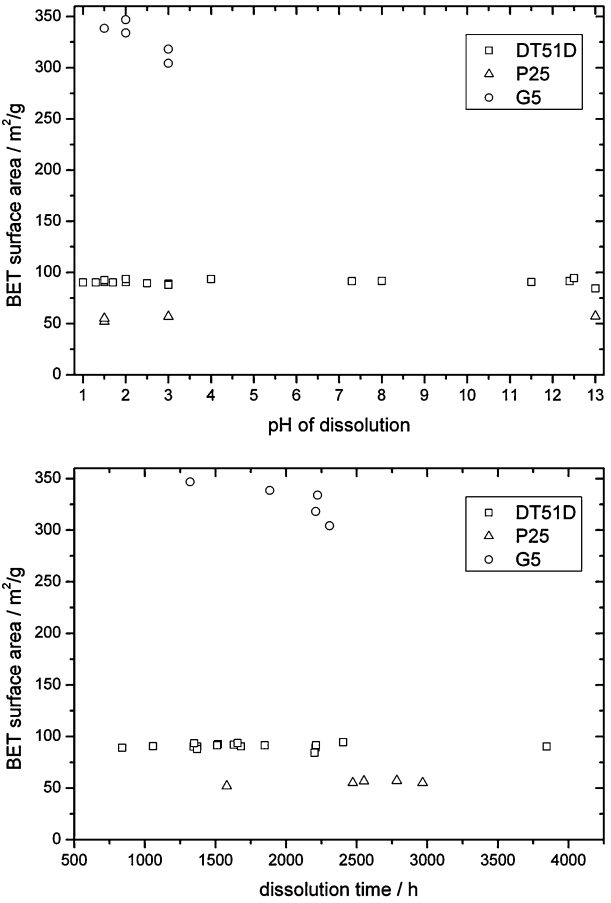

Fig. 6 BET surface areas of DT51D, P25, G5 for different pH values and dissolution times

(i.e., $n = 0$ to 5), it turns out that species with $n = 0$, 1 do not need to be considered. The titanium hydroxo complexes are connected via consecutive hydrolysis reactions that are dependent on pH:

$$[\mathrm{Ti(OH)}_n]^{(4-n)+} \leftrightarrows [\mathrm{Ti(OH)}_{n-1}]^{(5-n)+} + \mathrm{OH}^- \tag{5}$$

As only the total amount of titanium dissolved as function of the dissolution pH is known, and there are four unknown equilibrium constants (including the solubility product of TiO_2), Eq. 4 is an under-determined formula. That is, there is no unique solution. Therefore the fitting procedure (using the Levenberg-Marquardt algorithm; all calculations performed with the computer algebra system Mathematica [37]) was done with initial estimated values for the equilibrium constants of stepwise hydrolysis. These estimates were obtained from a preceding modelling of the dependence of titanium(IV) solubilities on pH over distinct pH-ranges, where the simplification can be made that only two species are prominent and therefore a determined (but approximate) equation is obtainable for the pH dependence of the total titanium(IV) concentration. Reasonable results are achieved by using this procedure. The same procedure was also applied for determining the cumulative hydrolysis constants. The cumulative equilibrium constants determined by fitting the solubility data of P25,

Table 4 Cumulative hydrolysis constants of titania ($I = 0$; 298 K) derived from solubility measurements of different industrially produced titanium dioxide nanoparticles

Reaction	$\log_{10} K$	Confidence interval 95%
P25 ($N = 35$ data points)		
$TiO_2 + 2H^+ \leftrightarrows Ti(OH)_2^{2+}$	−3.55	−3.91 to − 3.19
$TiO_2 + H^+ + H_2O \leftrightarrows Ti(OH)_3^+$	−6.15	−7.37 to − 4.93
$TiO_2 + 2H_2O \leftrightarrows Ti(OH)_4$	−9.02	−9.41 to − 8.63
$TiO_2 + 3H_2O \leftrightarrows Ti(OH)_5^- + H^+$	−19.83	−20.05 to − 19.61
DT51D ($N = 18$)		
$TiO_2 + 2H^+ \leftrightarrows Ti(OH)_2^{2+}$	−3.56	−3.80 to − 3.36
$TiO_2 + H^+ + H_2O \leftrightarrows Ti(OH)_3^+$	−5.93	−6.50 to − 5.36
$TiO_2 + 2H_2O \leftrightarrows Ti(OH)_4$	−9.07	−9.33 to − 8.81
$TiO_2 + 3H_2O \leftrightarrows Ti(OH)_5^- + H^+$	−19.78	−20.05 to − 19.52
G5 ($N = 32$)		
$TiO_2 + 2H^+ \leftrightarrows Ti(OH)_2^{2+}$	−2.88	−2.97 to − 2.80
$TiO_2 + H^+ + H_2O \leftrightarrows Ti(OH)_3^+$	−6.27	−5.30 to − 7.23
$TiO_2 + 2H_2O \leftrightarrows Ti(OH)_4$	−9.06	−9.16 to − 8.95
$TiO_2 + 3H_2O \leftrightarrows Ti(OH)_5^- + H^+$	−20.14	−20.23 to − 20.04

DT51D and G5, corrected for activity effects of the supporting electrolyte system according to Davies equation (Eq. 6) [38], are summarized in Table 4. The confidence intervals presented there are obtained by nonlinear fitting the overall experimental solubility data according to Eq. 4, taking the activity coefficients into account as calculated according to Davies empirical approximate equation (Eq. 6). In Eq. 6, γ_i represents the activity coefficient of the aqueous species i of charge z_i; I denotes the ionic strength and $A = 0.5102$ at 25 °C.

$$\log_{10} \gamma_i = -Az_i^2 \left(\frac{\sqrt{I}}{1+\sqrt{I}} - 0.3I \right) \tag{6}$$

The aqueous speciation shown in Fig. 7 can be calculated from the equilibrium constant data given in Table 5. It can be seen from the experimentally obtained equilibrium constants (Tables 4 and 5) and the solubility data (Fig. 5) that the species $Ti(OH)_2^{2+}$ (or TiO^{2+}) is prominent in the acidic pH range and that it determines the solubility of titania under these conditions. In the intermediate pH range of 3 to 11, the solubility of titania is about 1×10^{-9} mol·L^{-1} (at 0.1 mol·L^{-1} NaCl), where the neutral complex ion $Ti(OH)_4$ is predominant. At very alkaline conditions the solubility data indicate the formation of an anionic complex ion, $Ti(OH)_5^-$ (or $HTiO_3^-$).

The effect of the degree of hydroxylation on the solubility of titanium oxide is obvious when comparing samples DT51D, G5, P25 with TRONOX and TIPO. The sample TIPO was prepared by the hydrolysis of 5 mL titanium tetraisopropoxide (TTIP) in 50 mL aqueous solution (containing about 0.1 mol·L^{-1} NaCl) at the appropriate dissolution pH (adjusted by addition of small volumes of HCl or NaOH). Instantly after the addition of TTIP to the aqueous solution, a precipitate is formed (mainly an amorphous solid with small fractions of crystallites of rutile or anatase phase, as revealed by XRD after separation). After 170 hours following the initial hydrolysis of TTIP, the concentration of titanium(IV) dissolved in the supernatant solutions was determined. It was found that these solutions are supersaturated with Ti(IV) compared with solutions in equilibrium with crystalline titanium dioxide

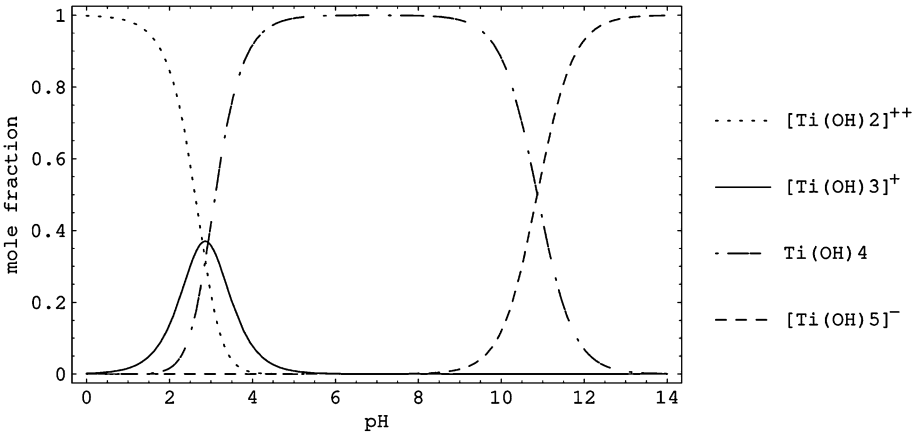

Fig. 7 Speciation of Ti(IV) in solutions in contact with solid titania (assuming mononuclear hydroxo complexes of titanium are the only species present) and its dependence on pH (25 °C, $I = 0$)

Table 5 Proposed stepwise and cumulative equilibrium constants for the hydrolysis of titania solutions ($I = 0$; 298 K) derived from solubility measurements (see Figs. 5 to 7)

	Mean value of $\log_{10} K$	Standard deviation of $\log_{10} K$
$Ti(OH)_2^{2+} + OH^- \leftrightarrows Ti(OH)_3^+$	12.15	0.43
$Ti(OH)_3^+ + OH^- \leftrightarrows Ti(OH)_4$	11.05	0.20
$Ti(OH)_4 + OH^- \leftrightarrows Ti(OH)_5^-$	2.91	0.19
$TiO_2 + 2H^+ \leftrightarrows Ti(OH)_2^{2+}$	−3.33	0.39
$TiO_2 + H^+ + H_2O \leftrightarrows Ti(OH)_3^+$	−6.12	0.17
$TiO_2 + 2H_2O \leftrightarrows Ti(OH)_4$	−9.05	0.03
$TiO_2 + 3H_2O \leftrightarrows Ti(OH)_5^- + H^+$	−19.92	0.20

(anatase). The uncalcined titanium hydrous oxide TRONOX (70% amorphous phase) also shows increased solubility compared to crystalline titania (P25, DT51D), see Fig. 5. The freshly prepared sample TIPO is more soluble than the uncalcined hydrous oxide TRONOX (dried at 110 °C), whereas crystalline titanium dioxide nanoparticles have the lowest solubility. Therefore, we can conclude that in dissolution experiments with samples that have high amorphous phase content and degree of hydroxylation, higher aqueous titanium(IV) solubilities are observed. It is established that oxides with very hydroxylated surfaces show higher solubilities compared to ones with less hydroxylated ones. In general, an amorphous form of a certain compound will have higher solubility than a well crystallized solid.

It should be emphasized that, when comparing or reporting solubilities, the effects of dissolution time (attainment of dissolution equilibria), primary particle size (Kelvin effect) and of hydroxylation and hydration of the solid phase should be taken into account.

We propose to use the mean of the equilibrium constants for the respective hydrolysis reaction of the three crystalline titania samples (P25, DT51D, G5) under consideration as the appropriate equilibrium constants for the hydrolysis of titania in general (Table 5). The standard deviations of the mean $\log_{10} K$ values that are calculated from the respective equilibrium constants for the three datasets can will also be used as an estimate for the errors of the hydrolysis constants presented here.

Table 6 Comparison of Gibbs energies for the hydrolysis of titanium hydroxo species reported by different authors

Reaction	$\Delta_r G^0$/kJ·mol^{-1}			
	This work	Ziemniak et al. [17]	Knauss et al. [18]	Nabivanets et al. [24]
$Ti(OH)_2^{2+} + OH^- \leftrightarrows Ti(OH)_3^+$	-69.3 ± 2.5	-66.8	–	-71.3
$Ti(OH)_3^+ + OH^- \leftrightarrows Ti(OH)_4$	-63.0 ± 1.1	-69.0	-69.5	-62.8
$Ti(OH)_4 + OH^- \leftrightarrows Ti(OH)_5^-$	-16.6 ± 1.1	-9.4 ± 1.2	-11.5	–
$TiO_2 + 2H^+ \leftrightarrows Ti(OH)_2^{2+}$	19.0 ± 2.2	27.3	–	–
$TiO_2 + H^+ + H_2O \leftrightarrows Ti(OH)_3^+$	34.9 ± 1.0	40.5	33.3	–
$TiO_2 + 2H_2O \leftrightarrows Ti(OH)_4$	51.63 ± 0.17	51.40 ± 0.23	43.5	–
$TiO_2 + 3H_2O \leftrightarrows Ti(OH)_5^- + H^+$	113.7 ± 1.1	121.9	112.0	–

4 Conclusions

The pH-dependent equilibrium solubility of titanium dioxide at 25 °C has been determined as approximated by the long-term solubilities (≥500 h) of industrially produced anatase samples. The quantitative determination of dissolved titanium(IV) has been carried out with AdSV in the mandelic acid–potassium chlorate system [28] and the reproducibility and accuracy of this method, as well as an appropriate sampling procedure, have been established [29].

Titania shows (0.1 mol·L^{-1} NaCl) solubilities as low as about 1 nmol·L^{-1} at 25 °C in the intermediate pH range (pH = 3 to 11), whereas solubilities in the range of 1 to 2 μmol·L^{-1} are observed at about pH = 1. The standard Gibbs energies for the stepwise hydrolysis reactions of titanium hydroxyl complexes, calculated from the equilibrium constants as well as existing literature data, are summarized in Table 6.

If necessary, data for the Gibbs energies of reaction were converted using the standard Gibbs energies of formation $\Delta_f G^0(H_2O, l) = -237.19$ kJ·mol^{-1} and $\Delta_f G^0(OH^-, aq) = -157.3$ kJ·mol^{-1} [17, 36]. The standard Gibbs energy $\Delta_r G^0 = (51.63 \pm 0.17)$ kJ·mol^{-1} for the dissolution of TiO_2, needed for calculating the Gibbs energy of formation of the aqueous species $Ti(OH)_4$, is in very good agreement with the value reported by Ziemniak et al. for the dissolution of rutile. In our experiments, no significant differences in the aqueous solubility of anatase and rutile (experiments at pH = 1.5/1.7/2.0) were observed. The standard Gibbs energies for stepwise hydrolysis of titanium hydroxo species obtained in this study are in reasonable agreement with previous results (see Table 6). The solubility product of titania determined in this work is $10^{-9.05 \pm 0.03}$. The degree of hydroxylation of the titanium (hydrous) oxide phase, besides the size-effects, strongly influences the observed aqueous solubilities. The equilibrium dissolution data for titania nanoparticles in sodium chloride solutions reported here provide an estimate of baseline solubility of TiO_2 in an aqueous environment.

Acknowledgements The XRD measurements were carried out by Dr. B. Müller of Friedrich-Schiller-University Jena. This is gratefully acknowledged.

References

1. Grätzel, M.: Photoelectrochemical cells. Nature **414**, 338–344 (2001). doi:10.1038/35104607

2. Zhang, Z., Wang, C., Zakaria, R., Ying, J.Y.: Role of particle size in nanocrystalline TiO_2-based photocatalysts. J. Phys. Chem. B **102**, 10871–10878 (1998). doi:10.1021/jp982948+
3. Holleman, A.F., Wiberg, N.: Lehrbuch der Anorganischen Chemie/Holleman-Wiberg. de Gruyter, Berlin/New York (1995)
4. Borm, P., Klaessig, F.C., Landry, T.D., Moudgil, B., Pauluhn, J., Thomas, K., Trottier, R., Wood, S.: Research strategies for safety evaluation of nanomaterials, Part V: Role of dissolution in biological fate and effects of nanoscale particles. Toxicol. Sci. **90**, 23–32 (2006). doi:10.1093/toxsci/kfj084
5. Oberdörster, G., Oberdörster, E., Oberdörster, J.: Nanotoxicology: an emerging discipline evolving from studies of ultrafine particles. Environ. Heal. Perspect. **113**, 823–839 (2005)
6. Nel, A., Xia, T., Mädler, L., Li, N.: Toxic potential of materials at the nanolevel. Science **311**, 622–627 (2006). doi:10.1126/science.1114397
7. Finnegan, M.P., Zhang, H., Banfield, J.F.: Anatase coarsening kinetics under hydrothermal conditions as a function of pH and temperature. Chem. Mater. **20**, 3443–3449 (2008). doi:10.1021/cm071057o
8. Jolivet, J., Cassaignon, S., Chanéac, C., Chiche, D., Tronc, E.: Design of oxide nanoparticles by aqueous chemistry. J. Sol-Gel Sci. Technol. **46**, 299–305 (2008). doi:10.1007/s10971-007-1645-4
9. Testino, A., Bellobono, I.R., Buscaglia, V., Canevali, C., D'Arienzo, M., Polizzi, S., Scotti, R., Morazzoni, F.: Optimizing the photocatalytic properties of hydrothermal TiO_2 by the control of phase composition and particle morphology. A systematic approach. J. Am. Chem. Soc. **129**, 3564–3575 (2007). doi:10.1021/ja067050+
10. Reyes-Coronado, D., Rodríguez-Gattorno, G., Espinosa-Pesqueira, M.E., Cab, C., de Coss, R., Oskam, G.: Phase-pure TiO_2 nanoparticles: anatase. Brookite and rutile. Nanotechnology **19**, 145605 (2008) (10 pp.)
11. Sugimoto, T., Zhou, X., Muramatsu, A.: Synthesis of uniform anatase TiO_2 nanoparticles by gel-sol method 1. Solution chemistry of $Ti(OH)_n^{(4-n)+}$ complexes. J. Colloid Interface Sci. **252**, 339–346 (2002). doi:10.1006/jcis.2002.8454
12. Pottier, A., Cassaignon, S., Chanéac, C., Villain, F., Tronc, E., Jolivet, J.: Size tailoring of TiO_2 anatase nanoparticles in aqueous medium and synthesis of nanocomposites. Characterization by Raman spectroscopy. J. Mater. Chem. **13**, 877–882 (2003). doi:10.1039/b211271j
13. Atashfaraz, M., Niassar, M.S., Ohara, S., Minami, K., Umetsu, M., Naka, T., Adschiri, T.: Effect of titanium dioxide solubility on the formation of $BaTiO_3$ nanoparticles in supercritical water. Fluid Phase Equilib. **257**, 233–237 (2007). doi:10.1016/j.fluid.2007.03.025
14. Schmidt, J., Vogelsberger, W.: Dissolution kinetics of titanium dioxide nanoparticles: the observation of an unusual kinetic size effect. J. Phys. Chem. B **110**, 3955–3963 (2006). doi:10.1021/jp055361l
15. Vogelsberger, W., Schmidt, J., Roelofs, F.: Dissolution kinetics of oxidic nanoparticles: the observation of an unusual behaviour. Colloids Surf. A Physicochem. Eng. Asp. **324**, 51–57 (2008). doi:10.1016/j.colsurfa.2008.03.032
16. Roelofs, F., Vogelsberger, W.: Dissolution kinetics of nanodispersed γ-alumina in aqueous solution at different pH: unusual kinetic size effect and formation of a new phase. J. Colloid Interface Sci. **303**, 450–459 (2006). doi:10.1016/j.jcis.2006.08.016
17. Ziemniak, S.E., Jones, M.E., Combs, K.E.S.: Solubility behavior of titanium(IV) oxide in alkaline media at elevated temperatures. J. Solution Chem. **22**, 601–623 (1993). doi:10.1007/BF00646781
18. Knauss, K.G., Dibley, M.J., Bourcier, W.L., Shaw, H.F.: Ti(IV) hydrolysis constants derived from rutile solubility measurements made from 100 to 300 °C. Appl. Geochem. **16**, 1115–1128 (2001). doi:10.1016/S0883-2927(00)00081-0
19. Antignano, A., Manning, C.E.: Rutile solubility in H_2O, H_2O–SiO_2, and H_2O–$NaAlSi_3O_8$ fluids at 0.7–2.0 GPa and 700–1000 °C: implications for mobility of nominally insoluble elements. Chem. Geol. **255**, 283–293 (2008). doi:10.1016/j.chemgeo.2008.07.001
20. Audétat, A., Keppler, H.: Solubility of rutile in subduction zone fluids, as determined by experiments in the hydrothermal diamond anvil cell. Earth Planet. Sci. Lett. **232**, 393–402 (2005). doi:10.1016/j.epsl.2005.01.028
21. Schuiling, R.D., Vink, B.W.: Stability relations of some titanium-minerals (sphene, perovskite, rutile, anatase). Geochim. Cosmochim. Acta **31**, 2399–2411 (1967). doi:10.1016/0016-7037(67)90011-7
22. Leturcq, G., Advocat, T., Hart, K., Berger, G., Lacombe, J., Bonnetier, A.: Solubility study of Ti,Zr-based ceramics designed to immobilize long-lived radionuclides. Am. Mineral. **86**, 871–880 (2001)
23. Liberti, A., Chiantella, V., Corigliano, F.: Mononuclear hydrolysis of titanium(IV) from partition equilibria. J. Inorg. Nucl. Chem. **25**, 415–427 (1963). doi:10.1016/0022-1902(63)80192-X
24. Nabivanets, B.I., Lukachina, V.V.: Hydroxy complexes of titanium(IV). Ukr. Khim. Zhur. **30**, 1123–1128 (1964)
25. Kelsall, G.H., Robbins, D.J.: Thermodynamics of Ti–H_2O–F(–Fe) Systems at 298 K. J. Electroanal. Chem. **283**, 135–157 (1990). doi:10.1016/0022-0728(90)87385-W

26. Comba, P., Merbach, A.: The titanyl question revisited. Inorg. Chem. **26**, 1315–1323 (1987). doi:10.1021/ic00255a024
27. Einaga, H.: Hydrolysis of titanium(IV) in aqueous (Na, H)Cl solution. Dalton Trans. **12**, 1917–1919 (1979)
28. Yokoi, K., van den Berg, C.M.G.: Determination of titanium in sea water using catalytic cathodic stripping voltammetry. Anal. Chim. Acta **245**, 167–176 (1991). doi:10.1016/S0003-2670(00)80217-2
29. Schmidt, J.: Charakterisierung des Löseverhaltens oxidischer Nanopartikel (TiO_2, ZrO_2, SiO_2) in wässrigen Systemen. Thesis, Friedrich-Schiller-Universität Jena, Jena, Germany (2008)
30. Kraus, W., Nolze, G.: PowderCell for Windows Version 2.4. Bundesanstalt für Materialforschung und –prüfung, Berlin (2000)
31. Barringer, E.A., Bowen, H.K.: High-purity, monodisperse TiO_2 powders by hydrolysis of titanium tetraethoxide. 1. Synthesis and physical properties. Langmuir **1**, 414–420 (1985). doi:10.1021/la00064a005
32. Löbbus, M., Vogelsberger, W., Sonnefeld, J., Seidel, A.: Current considerations for the dissolution kinetics of solid oxides with silica. Langmuir **14**, 4386–4396 (1998). doi:10.1021/la9712451
33. Kosmulski, M.: The significance of the difference in the point of zero charge between rutile and anatase. Adv. Colloid Interface Sci. **99**, 255–264 (2002). doi:10.1016/S0001-8686(02)00080-5
34. Hiemstra, T., Venema, P., Van Riemsdijk, W.H.: Intrinsic proton affinity of reactive surface groups of metal (hydr)oxides: the bond valence principle. J. Colloid Interface Sci. **184**, 680–692 (1996). doi:10.1006/jcis.1996.0666
35. Vogelsberger, W.: Thermodynamic and kinetic considerations of the formation and the dissolution of nanoparticles of substances having low solubility. J. Phys. Chem. B **107**, 9669–9676 (2003). doi:10.1021/jp030347z
36. Lencka, M.M., Riman, R.E.: Thermodynamic modeling of hydrothermal synthesis of ceramic powders. Chem. Mater. **5**, 61–70 (1993). doi:10.1021/cm00025a014
37. Wolfram, S.: Das Mathematica-Buch. Addison-Wesley/Longman, Bonn (1997)
38. Grenthe, I., Wanner, H., Östhols, E.: TDB-2, Guidelines for the Extrapolation to Zero Ionic Strength. OECD Nuclear Energy Agency (2000)